

Received: 2017.12.14  
Accepted: 2018.02.22  
Published: 2018.06.30

# Computed Tomographic Studies of Noncalcified Nodules Related to Neuroendocrine Lung Tumor Using <sup>68</sup>Gallium-Tagged Somatostatin Variant for Improvement in Diagnosis: A Non-Experimental, Non-Randomized, Cross-Sectional Study

Authors' Contribution:  
Study Design A  
Data Collection B  
Statistical Analysis C  
Data Interpretation D  
Manuscript Preparation E  
Literature Search F  
Funds Collection G

A 1 **Ketian Li**  
E 2 **Mingge Shen**  
BC 3 **Hang Geng**  
D 4 **Linyi Zheng**  
FG 2 **Yujie Cao**

1 Department of Nuclear Medicine, The First Affiliated Hospital of Jiamusi University, Jiamusi, Heilongjiang, P.R. China  
2 Department of Emergency Medicine, The First Affiliated Hospital of Jiamusi University, Jiamusi, Heilongjiang, P.R. China  
3 Department of Radiology, The First Affiliated Hospital of Jiamusi University, Jiamusi, Heilongjiang, P.R. China  
4 Department of Cardiology No. 1, The First Affiliated Hospital of Jiamusi University, Jiamusi, Heilongjiang, P.R. China.

**Corresponding Author:** Mingge Shen, e-mail: meoennynk2541@163.com  
**Source of support:** Departmental sources

**Background:** <sup>18</sup>Fluoro-fluorodeoxyglucose (FDG)- based positron-emission computed tomography (PET) has less specificity for noncalcified nodules (NNs). Somatostatin receptors affect the expression of normal and malignant cells. The purpose of the study was to compare the sensitivity, specificity, and accuracy of <sup>68</sup>Gallium-tagged DOTA-octreotate (Ga-tDO) with that of FDG PET for diagnosis of newly detected and/or untreated NNs in lung cancer patients.





**Material/Methods:** A total of 45 patients with lung cancer were included in the cross-sectional study and underwent Ga-tDO and FDG PET. We further confirmed observed outcomes by testing immune histochemical staining for subtype 2A of somatostatin receptor in a granuloma tissue array. The chi-square test was performed for sensitivity and specificity of predictive values among the 3 diagnostic modalities. McNemar's test was performed to compare accuracy between Ga-tDO and FDG PET. Results were considered significant at 95% confidence level.

**Results:** Ga-tDO had less sensitivity (69% vs. 89%) but more specificity (91% vs. 78%) than FDG PET. Ga-tDO and FDG PET were characterized as 36 and 6 and in 36 and 3 lesions as accurate and inaccurate, respectively. There was an insignificant difference between Ga-tDO and FDG PET regarding diagnostic accuracy (p=0.7). Dosimetry results showed that the lungs were one of the least critically affected organs.

**Conclusions:** Ga-tDO was more specific but less sensitive than FDG PET scanning and imaging.

**MeSH Keywords:** **Contrast Media • Contrast Sensitivity • Lung Neoplasms • Tomography, Emission-Computed**

**Full-text PDF:** <https://www.medscimonit.com/abstract/index/idArt/908545>

 2975  3  3  26



## Background

Lung cancer is the major contributor to cancer death in developing countries. The seriousness of lung cancer can be judged by the fact that 5-year (2002–2008) corresponding survival of all types of cancer including all stages was just 17% [1]. The main method for follow-up of smaller noncalcified lung nodules is by the computed tomography (CT) scan using Fleischner's criteria. Moreover, the timely follow up by the Radiology Department itself can provide valuable information about lung cancer patients to their consultants [2]. So far, <sup>18</sup>fluoro-fluorodeoxyglucose (FDG)- based positron-emission computed tomography (PET) has been established as a commonly used method for diagnosis of cancer and noncalcified nodules (NNs) [3]. However, its diagnosis accuracy for NNs is variable according to different conditions, which results in different accuracy due to false-negative and false-positive results [4,5]. False-positive results are obtained because of inflammatory or infectious foci, including the most blatant granulomatous bumps [6]. There are several reports showing that FDG-based PET has high sensitivity for NNs but has failed to specify NNs, especially granulomatous nodules [4,7] due to low true-negative percentage values. Hence, there is a need for a PET imaging contrast to improve discrimination of FDG in areas of endemic granulomatous lung bumps without compromising its high sensitivity in diagnosis.

Somatostatin receptors belong to the 7-transmembrane domain receptors family, which communicates changes in the secretion of hormones, the modulated death of cells, and regulation of proliferation of cells [8–10]. Because somatostatin receptors affect the expression of normal and malignant cells, or cancerous cells, research, especially in developing countries, uses the high-affinity somatostatin receptor variants in PET for imaging. With somatostatin receptor-expressing tumors, there is the possibility of improved spatial and contrast resolution of obtained scan results [11]. For patients who never underwent surgery and/or who did not respond well to typical treatments,  $\beta$ -emitting radionuclides-labeled somatostatin variants might be effective as directed radiotherapy, such as peptide receptor radionuclide therapy [4], as well as in the imaging of neuroendocrine tumors [12]. Somatostatin receptors variants have low signaling in normal lung tissues but have higher signaling in lung cancer as compared to the immune histochemical staining for subtype 2A of somatostatin receptor [13,14].

<sup>68</sup>Gallium-tagged DOTA-octreotate (Ga-tDO) is a conventional DOTA-conjugated peptide formed through chelation with a positron-emitting metal ion such as <sup>68</sup>Gallium for diagnosing, staging, and assessing treatment response [5] in PET imaging of somatostatin receptor-expressing tumors. In order to evaluate tumor dosimetry prior to administering it through peptide receptor radionuclide therapy, imaging-based radiopharmaceuticals have been used and found to have insignificant radiation-induced toxicity [7].

The primary aim of the present study was to compare the sensitivity, specificity, and accuracy of Ga-tDO with that of FDG for diagnosis of NNs, using PET scanning and imaging in newly detected and/or untreated NNs of lung cancer patients. The secondary aim of the study was to measure dosimetry for vital organs in case of Ga-tDO PET and to confirm observed outcomes by testing immune histochemical staining for subtype 2A of somatostatin receptor in a granuloma tissue array.

## Material and Methods

### Material

FDG was acquired from BV Cyclotron VU, Amsterdam, the Netherlands. Ethanol, sterile water, hydrochloric acid (HCl), formalin, and paraffin were purchased from Ranbaxy (Guangzhou China) Limited.

### Ethical consideration and consent to publish

The study had been registered in the research registry ([www.researchregistry.com](http://www.researchregistry.com)), UID No.: research registry 3419, dated 14 January 2015. The protocol (approval no. 974) of the study was approved by the First Affiliated Hospital of Jiamusi University Review Board for Radiological Research on Human Subjects with consideration of the STARD guidelines and the 2013 Declaration of Helsinki. We obtained written informed consent from all enrolled patients commencement of the study and permission to publish the work in any form (hard and soft) irrespective of time and language and recorded it in their electronic healthcare record (held at the Institute only). The study obtained consent under the approval of the Review Committee of the parent institute and referring institutes.

### Inclusion criteria

A total of 45 patients with lung cancer who were admitted to the Department of Oncology of the First Affiliated Hospital of Jiamusi University during February 2015 to July 2017 were included in the study. The study enrolled non-small cell lung cancer (NSCLC) subjects as adults aged more than 32 years old who had provided written informed consent to receive radiotherapy. Subjects had recently diagnosed lung cancer, untreated, diagnosed NNs (4–11 mm radius) of the lung and completed all the diagnostic protocols of the study.

### Exclusion criteria

Patients who refused to sign informed consent were excluded from the study. Patients who had been undergone thoracotomy in the last 60 days, received chemotherapy and/or radiotherapy

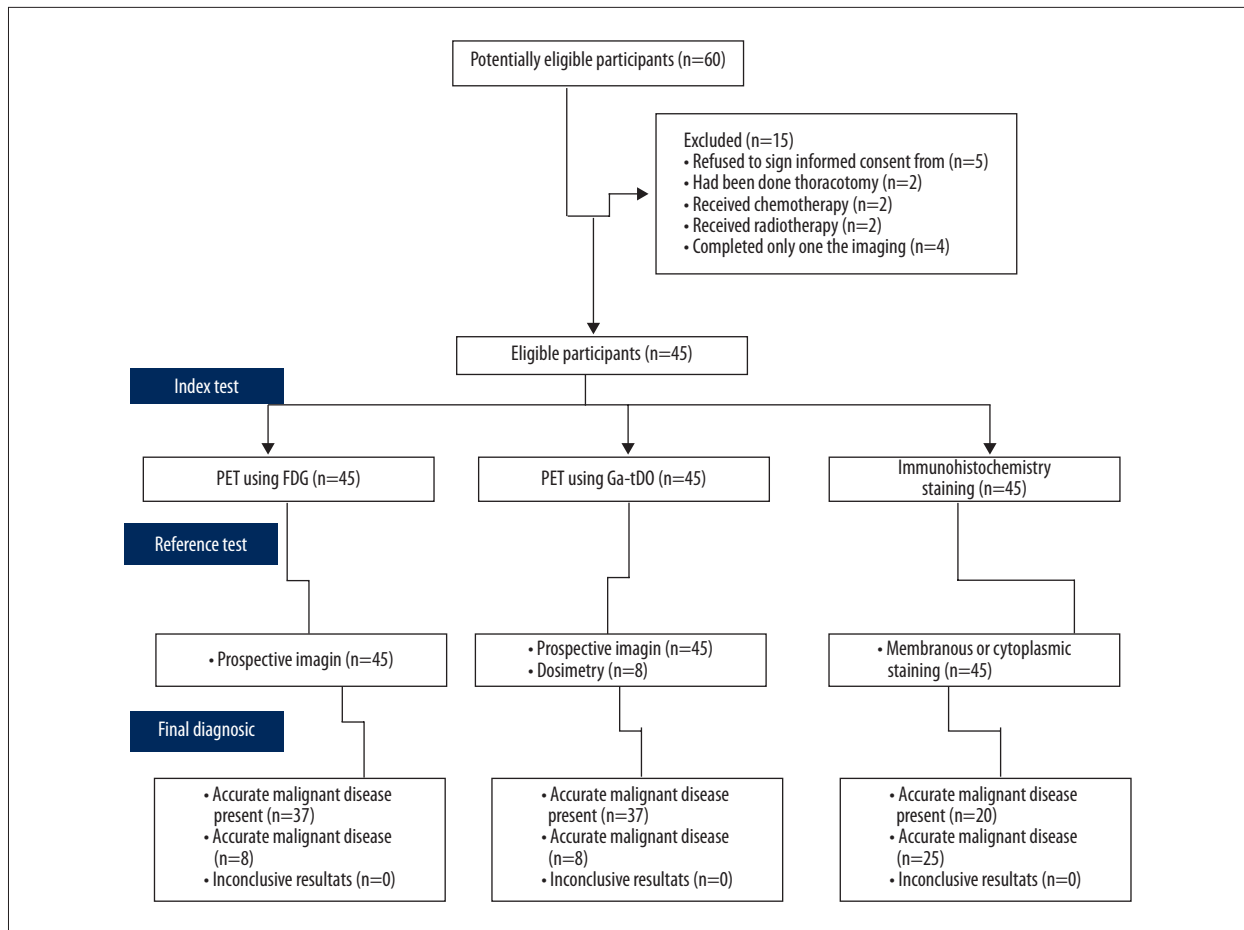


**Figure 1.** STARD flow chart of the non-randomized, non-experimental, cross-sectional study. PET – positron-emission computed tomography; Ga-tDO – <sup>68</sup>Gallium-tagged DOTA-octreotate; FDG – <sup>18</sup>Fluoro-fluorodeoxyglucose.

in the last year, and those who were able to complete only 1 of the imaging protocols of the study were excluded.

### Design of the study

All enrolled patients participated in the non-randomized, non-experimental, cross-sectional study. The STARD flow chart of the study is presented in Figure 1.

### PET

For the preparation of radiopharmaceuticals, the study used an on-the-spot <sup>68</sup>Ge/<sup>68</sup>Ga generator (Gallia Pharm®; model IGG100, Eckert & Ziegler Radiopharma, Berlin, Germany) after elution within 24 h before use with 0.1N HCl in 3 fractions. For dose preparation, we used the middle fraction and added the DOTA-octreotate solution (0.5 mL; 50 mg) using the protocol of ABX Advanced Biochemical Compounds (GmbH, Germany) followed by heating for 10 min at 100°C. Then, the vial was removed from heat and we added 4 mL of sterile water (for injection) after 5-min cooling and then filtered it into the final

collection vial using a membrane (0.22 mm). By using the same dose calibrator having the same geometry, the radionuclidic purity was determined, and Endosafe®-PTS™ (Charles River Laboratories International, USA) was used for bacterial endotoxin testing. A reversed-phase column (C-18, Waters Corp., USA) was used for reversed-phase liquid chromatography and it was used to confirm the radiochemical purity using solvents 0.001N HCl and then a 50: 50 mixture of ethanol: sterile water for 10 min each with the flow rate of 1 mL/min to reach >97% radiochemical purity [3].

The experiment followed standard-of-care for all FDG-infused protocols of PET scans. The patients were instructed to have limited physical exertion for 24 h and fast for at least 8 h. Insulin-dependent diabetics were instructed to withhold insulin for >8 h prior to the scanning. After activity adjustment for body weight, we injected 650 MBq of FDG (range 370–900 MBq; 17.1 mCi, range 10.1 mCi), and after 70 min we started the imaging. The average fasting blood sugar was kept at an average of 122 mg/dL (range, 69–272 mg/dL). For the imaging of Ga-tDO, each patient was intravenously injected with an average

of 190 MBq, range 170–219 MBq (6 mCi, range 5.2–7.5 mCi) and then imaged for an average of 70 min (range 52–122 min). The 8 patients were subjected to dosimetry measurements and the other patients emptied their bladders immediately after scanning. The study allowed a vertex to mild to high CT imaging using low-dose and without allowing the contrast, after placing the patients on the scanner table (Discovery VCT, GE Healthcare, Waukesha, WI, USA) and also kept the acquisition mode at 5 min at each bed position in 3-D imaging. The study time points were 48 min, 90 min, and 2 h for the beginning of emission just after injecting the Ga-tDO solution. A maximization algorithm with 2 iterations and 28 subsets was used for reconstruction of emission images using a 6-mm Z-axis filter (use condition: full width at half maximum). The study had stored final images using a 128×128 matrix set covering a 70-cm field of view. The interval between FDG imaging and Ga-tDO imaging was an average of 15 days (range 6–32 days) without any intermediate therapies. The cost of per dose of PET for an individual patient was also calculated.

### Dosimetry measurements

For this purpose, data obtained from 8 subjects were analyzed by following the aforementioned protocol of PET scans. Briefly, just before the injection of the Ga-tDO radiopharmaceutical, subjects voided their urinary bladders in order to eliminate any kind of biological activity, but they did not void again until after the completion of the entire dosimetry series. After placing the subjects on the scanner table, Ga-tDO PET scans were performed at 48 min after injection and keeping the rest conditions as mentioned before. For 7 subjects, we acquired at 3 time points but with the eighth subject, an arthritis patient, the study took only 2 points (at 66 min and 96 min after injection) due to intolerance for an additional emission. For reconstruction of emission images, the study followed the same procedure [15].

### Immunohistochemistry staining

The study performed immune histochemical staining (Biotrend, Schwabhausen, Germany) for subtype 2A of somatostatin receptor to examine its expression in malignant and benign nodules in order to further define it in lung cancer. It was performed on 6- $\mu$ m sections. The section was fixed in formalin and embedded on paraffin and interpreted visually under a digital biological microscope (45 × vision, PW-BK500LCD, Ningbo ProWay Optics & Electronics Co., Ltd., Zhejiang, China) [16]. A total of 45 lesions were subjected to immune histochemical staining and graded according to the intensity of cytoplasmic or sheath staining [17]. The staining technique used negative and positive controls for detection of tumor immunoreactivity. We further confirmed observed outcomes by testing immune histochemical staining for subtype 2A of somatostatin

receptor in a tissue array of granuloma, and observed logical findings to confirm NNs.

### Data analysis

We used a workstation (Xeleris 2™, GE Healthcare, USA) for the analysis of imaging results. In order to get SUV $\uparrow$  (the maximum standard uptake) values for normalization of primary tumors, including lean body mass, we measured 1-mL regions of interest. In the analysis, we excluded the unwanted portion of the CT and focused on the comparison of the uptakes of Ga-tDO and FDG for significant changes in detection of cancer. The cut-off of SUV $\uparrow$  was >2.5 for FDG for detection of cancer [18], but in the case of Ga-tDO, SUV $\uparrow$  >1.5 was chosen for lung cancer prevalence. The final diagnosis was determined by using either a 3-year chest CT follow-up or pathological tissue diagnosis. In order to assess the accuracy of diagnoses of cancer in all patients, contingency tables were created independently for both the protocols.

To obtain the dosimetry measurements data Ga-tDO, we drew volumes of interest around different parts of the body. In non-measured parts of the lower sides of the body, we evaluated the activity and found it was about 80%. To achieve a logical evaluation of the activity in the whole body, we divided the total measured counts by 80%. Thus, after multiplying the average voxel intensity with the volume of interest and using PET system calibration factor, we were able to get results related to dosimetry measurement. The dosimetry measurement results were combined in order to find its relation with disease diagnosis and we used related statistical calculations.

### Statistical analysis

Stata Vs 12 (Stata Corporation LLC, Texas, USA) was performed for all the analyses. The chi-square test was performed for sensitivity and specificity of predictive values among the 3 diagnostic modalities. McNemar's test was performed for accuracy between Ga-tDO PET and FDG PET [19]. Results were considered significant at 95% of confidence level.

## Results

The report of prospective imaging of 45 subjects with Ga-tDO and FDG PET is shown in Table 1. There were 23 malignant cases out of 45 lesions, with the average age of 63.6 years. Out of 23, 5 were metastatic transitional cell carcinoma cases and 18 were non-neuroendocrine cases. Two subjects had definite separate NNs and hence results of the diagnostic test were analyzed individually. Out of 45 lesions, 15 had a size larger than 32 mm. The average lesion size was 25 mm. The range of the lesion was in the range of 18–42 mm. Hence, out

**Table 1.** The report of prospective imaging using <sup>68</sup>Gallium-tagged DOTA-octreotate and <sup>18</sup>Fluoro-fluorodeoxyglucose based positron-emission the computed tomography.

S. No.	L. R.	Age (years)	Gen.	B. S.	G-SUV↑	F-SUV↑	Can.	Dia.	I.S.	Description
1	0.8	58	M	260	0.5	1.1	x	B	x	Fibrosis and necrosis-biopsy
2	0.5	50	F	96	0.6	0.6	x	B	x	Negative for malignant cells
3	0.9	60	M	237	0.4	1.0	x	B	x	RML-malignant cells present
4	0.7	49	M	92	0.5	0.5	x	B	x	Benign granuloma of bronchus-associated lymphoid tissue
5	0.8	76	M	111	0.6	4.5	√	M	x	Endobronchial biopsy-chronic inflammation
6	1.9	42	F	104	0.7	1.3	√	M	x	Negative for tumor or granuloma
7	0.8	>80	M	107	0.8	0.7	x	B	x	Consistent with histoplasmosis, negative for malignant cells
8	1.0	40	M	97	0.8	1.2	x	B	x	Nodules stable by 3 yr CT imaging. No cytology obtained
9	1.0	68	M	109	0.8	1.3	x	B	x	LUL-moderately to poorly differentiated A
10	0.6	46	M	104	0.8	1.4	x	B	x	Pulm nodules stable by 3 yr F-UCT imaging
11	1.1	50	M	112	0.8	5.2	√	A	x	Nodule was stable on 3 yr F-U by CT
12	0.5	69	F	117	0.9	1.4	√	A	x	SCC of the RUL
13	0.8	46	M	124	0.9	1.3	x	B	x	RUL well-differentiated A with mucinous features
14	1.0	53	M	125	0.9	5.8	x	B	x	1.5 cm dense fibrotic scar tissue
15	1.5	53	M	125	1.2	0.9	x	B	x	Nodule unchanged on 3 yr CT follow-up
16	1.8	62	F	119	1.1	1.3	√	M	x	Endobronchial biopsy-chronic inflammation,
17	1.7	64	F	108	0.8	4.6	√	M	x	Negative for tumor or granuloma
18	0.5	63	M	116	1.0	0.7	x	B	x	Non-small lung cancer, favor A
19	0.6	46	M	103	1.0	1.9	x	B	x	Bronchoscopic biopsy negative for malignant cells
20	2.0	59	M	114	1.2	4.0	x	B	x	Metastatic urothelial carcinoma (had 10 yr ago]
21	2.2	62	M	108	1.0	2.3	√	A	x	Right middle lobe A by pathologic diagnosis
22	0.9	66	M	102	1.1	0.9	√	A	x	poorly differentiated SCCA-RUL
23	0.7	64	F	104	1.2	0.8	x	B	x	right lower lobe-moderately differentiated A
24	1.9	49	M	112	1.4	3.0	x	B	x	LUL-moderately to poorly differentiated A
25	1.2	46	M	103	1.2	0.8	x	B	x	SCC by tissue diagnosis
26	2.1	57	M	97	1.2	3.5	x	B	x	Benign fibrosis by tissue diagnosis
27	1.5	68	F	99	1.8	2.9	x	B	x	RML-malignant cells present,
28	1.8	70	M	98	1.3	5.1	√	A	x	Poorly differentiated A via core biopsy
29	0.5	72	M	89	1.4	2.2	x	B	√	SCC by tissue diagnosis, right lower lobe
30	2.7	71	M	121	2.1	4.0	√	M	√	Broncholith noted in bronchoscopy report
31	0.7	66	M	117	1.7	11.0	√	S	√	RUL-negative for malignant cells via CT biopsy

**Table 1 continued.** The report of prospective imaging using <sup>68</sup>Gallium-tagged DOTA-octreotate and <sup>18</sup>Fluoro-fluorodeoxyglucose based positron-emission the computed tomography.

S. No.	L. R.	Age (years)	Gen.	B. S.	G-SUV↑	F-SUV↑	Can.	Dia.	I.S.	Description
32	3.5	63	M	101	1.5	15.0	√	A	√	Four core biopsies-poorly differentiated
33	2.8	65	M	130	1.6	6.5	√	A	√	SCC of the left lower lobe,
34	1.8	67	M	241	1.8	5.6	√	S	√	Benign granuloma via F-U imaging results.
35	1.0	62	M	169	2.4	5.2	√	S	√	Patient declined biopsy and elected CT follow-up.
26	3.6	60	M	88	1.9	6.1	x	B	√	RML-malignant cells present,
37	0.5	64	M	109	2.0	2.9	x	B	√	Metastatic urothelial carcinoma (had 10 yr ago]
38	1.9	73	M	102	2.1	5.1	√	A	√	Bronchus-associated lymphoid tissue
39	3.5	62	M	88	2.1	11.2	√	S	√	Endobronchial biopsy-chronic inflammation
40	1.2	78	M	136	2.5	5.0	√	S	√	Rare fungal yeasts, consistent with histoplasmosis
41	1.5	65	M	141	2.5	15.3	√	S	√	No cytology obtained
42	0.7	64	M	110	2.6	9.7	√	A	√	LUL-moderately to poorly differentiated A
43	1.1	65	M	71	3.2	13.9	√	S	√	Pulm nodules stable by 3 yr F-UCT imaging
44	1.5	59	M	93	3.4	3.7	√	S	√	RLL-negative for malignant cells via CT biopsy
45	3.0	72	M	112	3.8	13.6	√	S	√	RUL well-differentiated A with mucinous features

S. No – subject Number; L. R. – lesion radius (in cm); Gen. – Gender; B. S. – blood sugar (after fasting) (in mg/dL); G-SUV↑ – standard uptake value (maximum) for Ga-tDO; F-SUV↑ – standard uptake value (maximum) for FDG; Can. – cancer: √ – yes; x – no; Dia. – diagnosis; I. S. – Ga-tDO based immunohistochemically staining for subtype 2A of somatostatin receptor: positivity – √; negativity – x; B – benign; M – metastatic lung nodule from lung cancer; A – adenocarcinoma of the lung; S – squamous cell lung cancer; M – Male; F – Female; SCC – squamous cell carcinoma; F-U – follow-up; LUL – left upper lobe; RUL – right upper lobe; LUL – lower upper lobe; RML – right middle lobe; CT – computed tomography; n=45; Ga-tDO – <sup>68</sup>Gallium-tagged DOTA-octreotate based PET; FDG – <sup>18</sup>Fluoro-fluorodeoxyglucose based PET; PET – positron-emission computed tomography.

of 45 patients, the study reported 18 primary lung cancers, 5 patients with a metastatic nodule, and 22 benign nodules.

Ga-tDO was less sensitive (69% vs. 89%) but more specific (91% vs. 78%) than FDG (Table 2). When we compared the tests to check their ability to differentiate benign disease from malignancy, we found that they characterized the same 36 lesions accurately and 3 lesions inaccurately. Out of these 3 inaccurately classified lesions, 2 were partially differentiated adenocarcinoma and were false-negatives by both tests and the other one had been characterized as a benign lesion detected as a false-positive by both types of PET. Additionally, out of 3 malignant lesions, 1 metastatic case and 2 adenocarcinomas were classified inaccurately by Ga-tDO and accurately by FDG. For correlation of immunohistochemistry with imaging, we successfully characterized the primary tumor in tissue

lesions of 20 patients. Immune histochemical staining failed in the specification of lung cancers in all patients, although the study achieved Ga-tDO uptake. We also found that there was limited staining observed, which was supported by assessment of the stroma and/or inflammatory cells. Seven out of 11 NSCLC cases had a positive response to immune histochemical staining for subtype 2A of somatostatin receptor. However, all 4 benign lesions had a negative response to it (Figure 2).

We found an insignificant difference between Ga-tDO PET and FDG PET regarding diagnostic accuracy (p=0.7, Figure 3).

We also found that overall uptake of contrast agent in normal and mediastinal tissues of the lung was low and was the same between Ga-tDO PET and FDG PET. There was intense FDG uptake but adverse Ga-tDO uptake in 2 inflammatory benign

**Table 2.** Comparison of <sup>68</sup>Gallium-tagged DOTA-octreotate and <sup>18</sup>Fluoro-fluorodeoxyglucose based positron-emission the computed tomography in terms of their performances.

Percentage characteristic features	Ga-tDO (95% CI)	FDG (95% CI)
Negative predictive value	79.4 (56.9–91.9)	93.2 (75.9–99.8)
Positive predictive value	92.1 (67.4–98.4)	82.9 (66.9–95.2)
Sensitivity	69.4 (55.6–85.9)	89.3 (56.8–97.2)
Specificity	91.2 (71.2–99.7)	77.9 (64.0–90.4)
The area under the receiver operating characteristic curve	0.86 (0.73–0.96)	0.89 (0.79–0.98)

n=45; CI – confidence interval; Ga-tDO – <sup>68</sup>Gallium-tagged DOTA-octreotate based PET; FDG – <sup>18</sup>Fluoro-fluorodeoxyglucose based PET; PET – positron-emission computed tomography. The cut-off of the maximum standard uptake was >2.5 for FDG and >1.5 for Ga-tDO for detection of cancer.

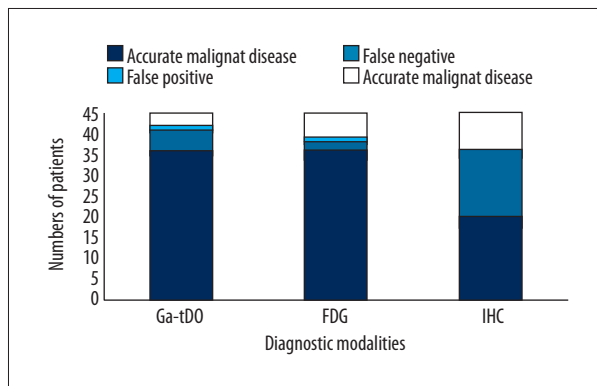


**Figure 2.** Comparisons of results for sensitivity and specificity of predictive values of different diagnostic modalities. The chi-square test was used for statistical analysis. A  $p < 0.05$  was considered as significant. No significant discrimination regarding results between Ga-tDO and FDG ( $p = 0.091$ ). Ga-tDO – <sup>68</sup>Gallium-tagged DOTA-octreotate-based PET; FDG – <sup>18</sup>Fluoro-fluorodeoxyglucose based PET; INC – immunohistochemistry staining; PET – positron-emission computed tomography.

nodules. Statistically equivalent results for Ga-tDO PET and FDG PET scans regarding the staging of lung cancer were reported.

We found that for Ga-tDO, the least critically affected organ was the skin, followed by breasts and muscle, and the lungs were among the least critically affected organs (Table 3).

## Discussion

During the study, FDG PET failed in the characterization of 2 benign lesions, but both had been accurately classified by Ga-tDO PET. Diagnosis of NNs is challenging. CT images and immunohistochemistry are used to aid in the diagnosis [2]. <sup>68</sup>Ga was produced from the generator and yielded similar accuracy compared to FDG [20]. However, FDG PET is well-established

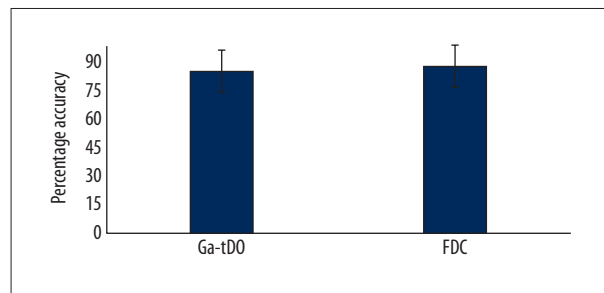


**Figure 3.** Comparison of accuracy different diagnostic modalities. Ga-tDO – <sup>68</sup>Gallium-tagged DOTA-octreotate-based PET. No significant discrimination for overall diagnostic accuracy between 2 imaging techniques ( $p = 0.7$ ). FDG – <sup>18</sup>Fluoro-fluorodeoxyglucose based PET; PET – positron-emission computed tomography. McNemar's test was used for statistical analysis. A  $p < 0.05$  was considered as significant.

for use in the characterization of NNs [3]. In respect to the results of the study, the finding had uniquely focused on work in an area with huge local granulomatous bumps and demonstrated the equivalency of Ga-tDO PET with FDG PET in the diagnosis and staging of NSCLC, along with a diagnosis of a malignant NNs in terms of accuracy. Additionally, it is noteworthy that no critical events were found in terms of delayed toxicity from Ga-tDO, even after long-term follow-up.

Ga-tDO is freely available at low cost. FDG has limitations of availability and high cost [21]. The investigation established that Ga-tDO PET is better than FDG PET.

In the present study, except for some cases with discrepant findings, in most of the cases, FDG PET and Ga-tDO PET were statistically equivalent for characterization of lung cancer, and overall accuracy for each of the radiopharmaceuticals was 89%. In an earlier report, FDG PET was found to be more specific (71% vs. 51%) and equally sensitive (96% vs. 94%) with <sup>99m</sup>Tc-depreotide SPECT (TSPECT) imaging regarding the staging of NSCLC in 157 subjects [22]. In another report, including

**Table 3.** Detailed dosimetry measurements of eight patients with respect to vital organs.

Targeted organ	Estimated dose of radiation (in mSv/MBq)										
	Patients								Avg	SD	CV
	1	2	3	4	5	6	7	8			
Spleen	0.211	0.221	0.120	0.385	0.396	0.216	0.405	0.364	0.289	0.129	43.2
Urinary bladder wall	0.112	0.122	0.180	0.121	0.101	0.169	0.0212	0.186	0.150	0.0621	48.1
Kidneys	0.114	0.143	0.112	0.123	0.103	0.0628	0.0655	0.0781	0.105	0.0294	31.8
Liver	0.0189	0.0173	0.0413	0.0594	0.0564	0.0475	0.0617	0.0427	0.0432	0.0122	31.8
Pituitary gland	0.0151	0.0131	0.122	0.0262	0.0234	0.0493	0.0229	0.0338	0.0382	0.0304	75.1
Thyroid	0.0264	0.0244	0.0363	0.00983	0.00979	0.0119	0.0122	0.0178	0.0186	0.0102	56.1
Pancreas	0.0156	0.0148	0.0139	0.0188	0.0167	0.0157	0.0176	0.0179	0.0164	0.00132	81.7
Adrenals	0.0158	0.0134	0.0151	0.0139	0.0156	0.0132	0.0169	0.0132	0.0146	0.000518	35.5
Small intestine	0.0181	0.0173	0.0142	0.0113	0.0137	0.0129	0.0139	0.0116	0.0141	0.00257	18.2
Stomach wall	0.0151	0.0147	0.0139	0.0138	0.0151	0.0124	0.013	0.0128	0.0139	0.000643	4.7
Ovaries	0.0143	0.0133	0.0149	0.0132	0.0142	0.0115	0.0111	0.0109	0.0129	0.000829	6.3
Heart wall	0.0131	0.0137	0.0112	0.0121	0.0119	0.0134	0.0117	0.011	0.0122	0.000390	3.19
Salivary glands	0.00225	0.00205	0.0237	0.00675	0.00698	0.0120	0.00712	0.0145	0.0119	0.00778	66.2
Lungs	0.0129	0.0111	0.0123	0.0102	0.0122	0.0110	0.0109	0.0102	0.0113	0.000345	3.01
Muscle	0.0112	0.0116	0.0110	0.0101	0.0102	0.0105	0.0104	0.0107	0.0107	0.000434	3.86
Testes	0.0111	0.0109	0.0112	0.0109	0.0101	0.0091	0.0102	0.00984	0.0104	0.000668	6.01
Breasts	0.0116	0.00986	0.00956	0.00952	0.00932	0.0111	0.00991	0.00965	0.01	0.000421	4.22
Skin	0.0113	0.00983	0.00987	0.00901	0.00959	0.00923	0.00933	0.00911	0.00964	0.000421	4.32

CV – coefficient of variation; SD – standard deviation; Avg – average.

114 patients, TSPECT imaging was used for solitary NNs and yielded 91% accuracy for the discrimination between malignant and benign lesions [23]. On the other hand, the work in which TSPECT imaging compared with FDG PET for diagnosis of NNs 0.8–3 cm in size, a non-significant difference was observed for both the methods [24]. To the best of our knowledge, there is only 1 study of 9 NSCLC, in which Ga-tDO was compared with FDG PET, and showed lower mean primary tumor SUV↑ in comparison to the latter (2.0 vs. 5.7) [3]. Regarding available literature, the study was a novel prospective assignment which successfully compares the outcomes of Ga-tDO and FDG PET scans of recently detected lung cancer patients or high-risk lung cancer patients having NNs.

The positive response of immune histochemical staining for subtype 2A of somatostatin receptor was found in the inflammatory cells or stroma type tissue lesions but not in cells of the tumor. This happened only because there is the possibility of some degree of neuroendocrine differentiation in one-third of NSCLC, as reported elsewhere [25]. An earlier report has mentioned that subtype 2A of somatostatin receptor is highly signaled on different types of benign cells like fibroblasts, the endothelium, and activated macrophages [26]. Besides, the study had found higher SUV↑ values for Ga-tDO for cancer (2.5) than benign (1.1). Similar results were found in the second case of FDG (8.6 vs. 2.1, respectively). In spite of the fact that immune histochemical staining for subtype 2A of somatostatin receptor was unreacted in all tumor cells but resulted in the uptake of Ga-tDO within the tumor stroma, it will



definitely inspire further investigation to reveal the interaction between lung cancer tumors and the microenvironment.

The prime limitation of the study was its small numbers of tissue samples. There was also an unexpectedly low number of granulomatous nodules due to the small study size along with incomplete tissue sampling. Male dominance in the study was another limitation to the work.

## Conclusions

This was a non-randomized, non-experimental, cross-sectional study of 45 patients having a total of 45 lesions.

## References:

1. Siegel RL, Miller KD, Jemal A: Cancer statistics. *Cancer J Clin*, 2015; 65: 5–29
2. Motiwala H, Bansal I, Goyal P et al: Do we really care about incidental lung nodules? – Review of atypical lung carcinoid and a proposal for systematic patient follow up. *Transl Lung Cancer Res*, 2017; 6(3): 387–92
3. Dimitrakopoulou-Strauss A, Georgoulas V, Eisenhut M et al: Quantitative assessment of SSTR2 expression in patients with non-small cell lung cancer using (68) Ga-DOTATOC PET and comparison with (18) F-FDG PET. *Eur J Nucl Med Mol Imaging*, 2006; 33: 823–30
4. Deppen SA, Blume JD, Kensing CD et al: Accuracy of FDG-PET to diagnose lung cancer in areas with infectious lung disease: A meta-analysis. *JAMA*, 2014; 312: 1227–36
5. Grogan EL, Deppen SA, Ballman KV et al: Accuracy of fluorodeoxyglucose-positron emission tomography within the clinical practice of the American College of Surgeons Oncology Group Z4031 trial to diagnose clinical stage I non-small cell lung cancer. *Ann Thorac Surg*, 2014; 97: 1142–48
6. Cuaron J, Dunphy M, Rimmer A: Role of FDG-PET scans in staging, response assessment, and follow-up care for non-small cell lung cancer. *Front Oncol*, 2013; 2: 208
7. Croft DR, Trapp J, Kernstine K et al: FDG-PET imaging and the diagnosis of non-small cell lung cancer in a region of high histoplasmosis prevalence. *Lung Cancer*, 2002; 36: 297–301
8. Callison JC Jr, Walker RC, Massion PP: Somatostatin receptors in lung cancer: From function to molecular imaging and therapeutics. *J Lung Cancer*, 2011; 10: 69–76
9. Bodmer D, Brand Y, Radojevic V: Somatostatin receptor types 1 and 2 in the developing mammalian cochlea. *Dev Neurosci*, 2012; 34: 342–53
10. Theodoropoulou M, Stalla GK: Somatostatin receptors: From signaling to clinical practice. *Front Neuroendocrinol*, 2013; 34: 228–52
11. De K, Banerjee I, Misra M: Radiolabeled new somatostatin analogs conjugated to DOMA chelator used as targeted tumor imaging agent: Synthesis and radiobiological evaluation. *Amino Acids*, 2015; 47: 1135–53
12. Herrmann K, Czernin J, Wolin EM et al: Impact of 68Ga-DOTATATE PET/CT on the management of neuroendocrine tumors: The referring physician's perspective. *J Nucl Med*, 2015; 56: 70–75
13. Tsuta K, Wistuba II, Moran CA: Differential expression of somatostatin receptors 1–5 in neuroendocrine carcinoma of the lung. *Pathol Res Pract*, 2012; 208: 470–74
14. Righi L, Volante M, Tavaglione V et al: Somatostatin receptor tissue distribution in lung neuroendocrine tumours: A clinicopathologic and immunohistochemical study of 218 'clinically aggressive' cases. *Ann Oncol*, 2010; 21: 548–55
15. Flechsig P, Frank P, Kratochwil C et al: Radiomic analysis using density threshold for FDG-PET/CT-based n-staging in lung cancer patients. *Mol Imaging Biol*, 2017; 19: 315–22
16. Papotti M, Bongiovanni M, Volante M et al: Expression of somatostatin receptor types 1–5 in 81 cases of gastrointestinal and pancreatic endocrine tumors. A correlative immunohistochemical and reverse-transcriptase polymerase chain reaction analysis. *Virchows Arch*, 2002; 440: 461–75
17. Kaemmerer D, Athellogou M, Lupp A et al: Somatostatin receptor immunohistochemistry in neuroendocrine tumors: Comparison between manual and automated evaluation. *Int J Clin Exp Pathol*, 2014; 7: 4971–80
18. Deppen S, Putnam JB Jr, Andrade G et al: Accuracy of FDG-PET to diagnose lung cancer in a region of endemic granulomatous disease. *Ann Thorac Surg*, 2011; 92: 428–32
19. Gupta M, Choudhury PS, Hazarika D, Rawal S: A comparative study of 68Gallium-prostate-specific membrane antigen positron emission tomography-computed tomography and magnetic resonance imaging for lymph node staging in high-risk prostate cancer patients: An initial experience. *World J Nucl Med*, 2017; 16: 186–91
20. Ebenhan T, Vorster M, Marjanovic-Painter B et al: Development of a single vial kit solution for radiolabeling of 68Ga-DKFZ-PSMA-11 and its performance in prostate cancer patients. *Molecules*, 2015; 20: 14860–78
21. Rusthoven KE, Koshy M, Paulino AC: The role of fluorodeoxyglucose positron emission tomography in cervical lymph node metastases from an unknown primary tumor. *Cancer*, 2004; 101: 2641–49
22. Kahn D, Menda Y, Kernstine K et al: The utility of 99mTc depreotide compared with F-18 fluorodeoxyglucose positron emission tomography and surgical staging in patients with suspected non-small cell lung cancer. *Chest*, 2004; 125: 494–501
23. Walker R, Deppen S, Smith G et al: 68Ga-DOTATATE PET/CT imaging of indeterminate pulmonary nodules and lung cancer. *PLoS One*, 2017; 12: e0171301
24. Halley A, Hugentobler A, Icard P et al: Efficiency of 18F-FDG and 99mTc-depreotide SPECT in the diagnosis of malignancy of solitary pulmonary nodules. *Eur J Nucl Med Mol Imaging*, 2005; 32: 1026–32
25. Howe MC, Chapman A, Kerr K et al: Neuroendocrine differentiation in non-small cell lung cancer and its relation to prognosis and therapy. *Histopathology*, 2005; 46: 195–201
26. Giandomenico V, Cui T, Grimelius L et al: Olfactory receptor 51E1 as a novel target for diagnosis in somatostatin receptor-negative lung carcinoids. *J Mol Endocrinol*, 2013; 51: 277–86

## Acknowledgements

All authors are thankful to all radiological and non-radiological staff of the First Affiliated Hospital of Jiamusi University, Jiamusi, Heilongjiang, China who made the study successful.